



Structural analysis of the active sites of dihydrofolate reductase from two species of *Candida* uncovers ligand-induced conformational changes shared among species

Janet L. Paulsen, Kishore Viswanathan, Dennis L. Wright*, Amy C. Anderson*

Department of Pharmaceutical Sciences, University of Connecticut, 69 N. Eagleville Rd., Storrs, CT 06269, USA

ARTICLE INFO

Article history:

Received 4 October 2012
Revised 20 December 2012
Accepted 2 January 2013
Available online 11 January 2013

Keywords:

Antifolate
DHFR
Protein flexibility
X-ray crystallography
Molecular dynamics

ABSTRACT

A novel strategy for targeting the pathogenic organisms *Candida albicans* and *Candida glabrata* focuses on the development of potent and selective antifolates effective against dihydrofolate reductase. Crystal structure analysis suggested that an essential loop at the active site (Thr 58-Phe 66) differs from the analogous residues in the human enzyme, potentially providing a mechanism for achieving selectivity. In order to probe the role of this loop, we employed chemical synthesis, crystal structure determination and molecular dynamics simulations. The results of these analyses show that the loop residues undergo ligand-induced conformational changes that are similar among the fungal and human species.

© 2013 Elsevier Ltd. All rights reserved.

The severe health risks presented by systemic fungal infections continue to produce significant increases in mortality and morbidity. *Candida* spp. are primary pathogenic organisms in systemic infections with *Candida albicans* accounting for approximately 50–70% of infections.^{1,2} However, *Candida glabrata*, associated with a high rate of mortality, now accounts for an increasing proportion of infections.^{3,4} Additionally, *C. glabrata* is less sensitive to commonly used antifungal agents such as fluconazole and other azoles.^{1,5} The development of new classes of antifungal agents with good potency against these *Candida* species is a high priority.

The vast majority of the current antifungal agents target the fungal cell wall or its biosynthesis, leaving many of the essential metabolic functions unexplored as therapeutic targets. One such essential enzyme, dihydrofolate reductase (DHFR), has long been appreciated as an effective target for antimicrobial therapy. As DHFR is also essential to human cells, an effective antifungal antifolate design must take advantage of differences in the pathogenic enzyme relative to the human enzyme. Over the past several years we have focused on the development of a novel class of antifolates characterized by a conserved diaminopyrimidine moiety linked through a propargylic spacer to a variable hydrophobic domain.^{6–11} Leads such as compound **1** (shown in Table 1) have been shown to function as inhibitors of *C. glabrata* (CgDHFR) and *C. albicans* DHFR (CaDHFR) as well as exhibit antifungal activity (MIC values

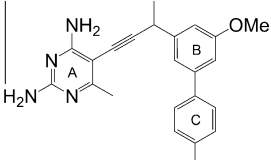
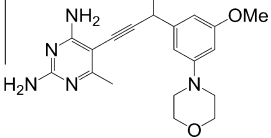
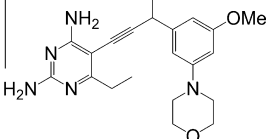
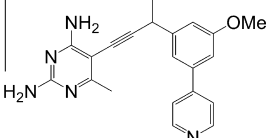
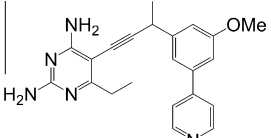
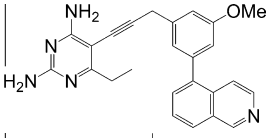
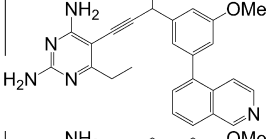
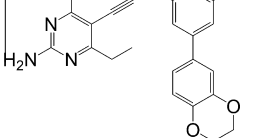
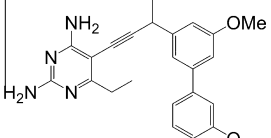
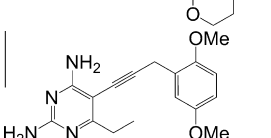
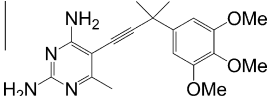
of 1.5 µg/mL) and thus are interesting as potential antifungal therapeutics.^{7,8,11} We have reported several crystal structures of CgDHFR and CaDHFR bound to NADPH and several members of this lead series.^{7,8,11} Analysis of these crystal structures has strongly suggested that residues in a loop at the fungal active site (Thr 58-Phe 66) may be displaced further from the active site relative to the analogous residues in the human structure (Thr 56-Asn 64), a property that may be advantageous for gaining selectivity in inhibitor design.

In order to investigate whether this critical loop truly plays an active role in determining the affinity of the propargyl-linked antifolates for the fungal and human enzymes, here we present an analysis of existing crystal structures of CgDHFR and CaDHFR bound to the propargyl-linked antifolates as well as four new ternary crystal structures of CgDHFR and CaDHFR bound to a recent generation of inhibitors possessing a heterocyclic moiety intended to improve solubility.¹² We then designed and synthesized four additional propargyl-linked antifolates with a bulkier, fused ring system intended to especially probe the flexibility of the loop. Crystal structures of CgDHFR and CaDHFR with one of these compounds emphasize the ligand-induced conformational changes observed with these more sterically demanding inhibitors. Finally, we carried out a detailed molecular dynamics study that focused on the loop regions of both the fungal and human enzymes. These MD results show that this loop in the active site is particularly flexible and while the loop undergoes ligand-induced conformational changes, these changes are similar across the three species.

* Corresponding authors. Tel.: +1 860 486 6145/9451; fax: +1 860 486 6857.

E-mail addresses: dennis.wright@uconn.edu (D.L. Wright), amy.anderson@uconn.edu (A.C. Anderson).

Table 1
Enzyme inhibition of CaDHFR, CgDHFR and human DHFR with propargyl-linked antifolates

ID	Structure	CaDHFR IC ₅₀ (nM) (selectivity)	CgDHFR IC ₅₀ (nM) (selectivity)	huDHFR IC ₅₀ (nM)
1		22 ± 1 (64)	0.60 ± 0.27 (2350)	1410 ± 15
2		21 ± 4 (19)	20 ± 3 (20)	400 ± 40
3		23 ± 4 (11)	22 ± 2 (11)	250 ± 4
4		61 ± 3 (25)	97 ± 9 (15)	1500 ± 80
5		60 ± 2 (22)	89 ± 8 (15)	1300 ± 10
12		71 ± 20 (0.84)	16 ± 1 (3.8)	60 ± 6
13		17 ± 5 (2.6)	11 ± 1 (4.1)	45 ± 3
18		78 ± 2 (1.8)	19 ± 4 (7.4)	140 ± 9
19		23 ± 2 (11)	18 ± 3 (14)	260 ± 20
20		100 ± 7 (13)	8.2 ± 1.3 (156)	1280 ± 15
21		33 ± 14 (9)	11 ± 2 (26)	290 ± 17

Over the past several years, we have reported eight CgDHFR and three CaDHFR crystal structures bound to NADPH and antifolates possessing a pyrimidinyl ring linked through the propargyl bridge

to substituted monophenyl or biphenyl systems.^{7,8,11} Analysis of these structures has been critical to improving the potency and selectivity of the inhibitors for the fungal enzymes. While there

are a few residue substitutions between the human and fungal enzymes, including Phe 31/Met 33[Ile 33], Val 115/Ile 122 and Asn 64/Phe 66 (Fig. 1A), a broad study of these fungal structures in comparison to structures of the human DHFR enzyme¹³ has suggested the intriguing possibility that selective inhibitors could be designed by taking advantage of conformational differences in a key active site loop found in both fungal pathogens (residues 63–66) as well as human DHFR (residues 61–64). Figure 1 shows a structural alignment of CaDHFR, CgDHFR and human DHFR (huDHFR) as well as a superposition of the two fungal enzymes bound to propargyl-linked antifolates with monophenyl moieties and the human enzyme bound to a pyridopyrimidine inhibitor.¹³ The structural comparison suggests that the loop in human DHFR (61–64) restricts the active site more profoundly than the corresponding loop in fungal DHFR (58–66) and that selective inhibitors may be designed with increased bulk at the distal ring to sterically interfere with the loop in human DHFR.

As we had observed that a third generation of compounds possessing heterocyclic ring systems at the distal position (ring C in structure 1) showed improved solubility,¹² we also evaluated these compounds as inhibitors of the fungal enzymes (Table 1). Overall, conversion of the phenyl ring in 1 to either aromatic or alicyclic heterocycles (2–5, 12, 13, 18, 19) results in an attenuation of enzyme inhibition (3- to 20-fold loss) and selectivity ratios. In order

to understand the structural basis of the reduced potency, we determined four ternary crystal structures: CgDHFR bound to 3 (PDB ID: 3ROA), CgDHFR bound to 5 (PDB ID: 3RO9), CaDHFR bound to 5 (PDB ID: 4H95) and CaDHFR bound to 1 (PDB ID: 4H97), as a comparator (crystallographic details in Supplementary data). Analysis of these structures shows that compounds 3 and 5, especially as bound to CgDHFR, reorient to bring the polar distal ring away from loop residues Pro 63 and Phe 66 and toward the solvent accessible surface, thus decreasing hydrophobic contacts (Fig. 2A). As previously noted, the loop residues appear to be flexible in CgDHFR with the position of the C α atoms of Pro 63 varying between 0.5 and 1.1 Å. Similarly, in the structures with CaDHFR bound to 1 and 5, the distance between Pro 63 C α atoms is 0.8 Å (Fig. 2B).

Our prior structural analysis suggested that increasing bulk at the distal C-ring position of the inhibitors may improve potency by increasing contacts with the fungal enzymes (specifically residues Pro 63 and Phe 66) while simultaneously improving selectivity by inducing steric interference with the human residues Pro 61 and Asn 64, which appeared to be closer to the inhibitors. This strategy relies on species-specific conformations of the loop in both enzymes. In order to evaluate this hypothesis, we first designed a focused docking library for evaluation *in silico*. The design involved the annulation of the distal C ring with the specification of

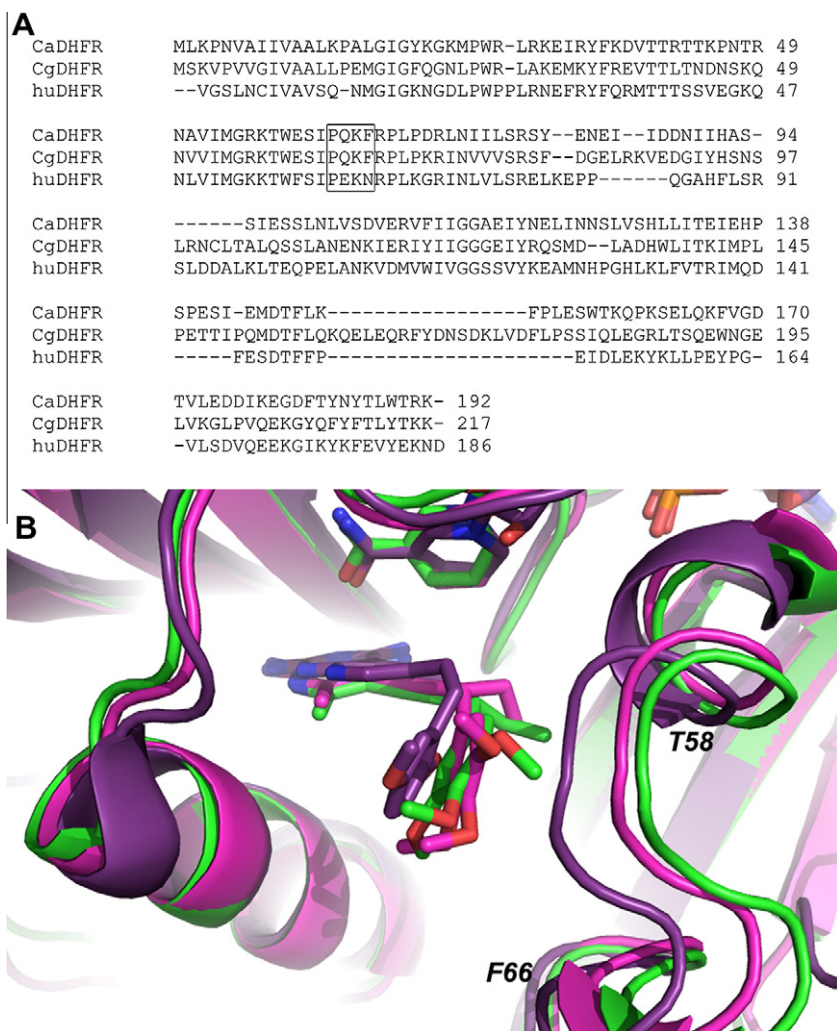


Figure 1. (A) Structural alignment of CaDHFR, CgDHFR and huDHFR with the loop residues boxed, (B) structural differences in the loop region of CaDHFR (green; PDB ID: 3QLR¹¹), CgDHFR (pink; PDB ID: 3QLX¹¹) and human DHFR (purple; PDB ID: 1PD8¹³).

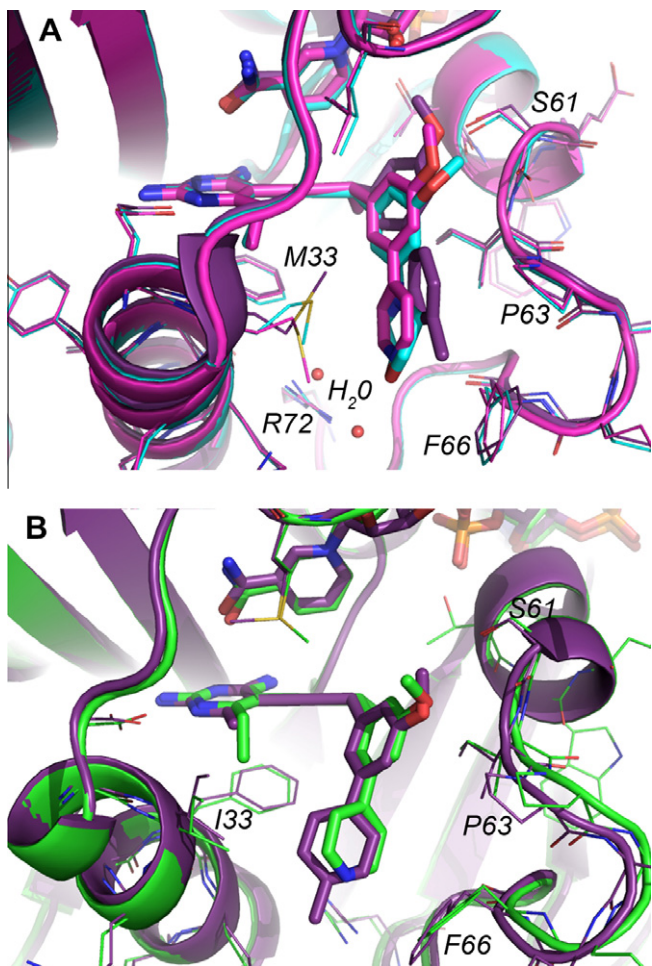


Figure 2. (A) CgDHFR in complex with **3** (cyan), **5** (pink) and **1** (purple), (B) CaDHFR in complex with **5** (green) and **1** (purple).

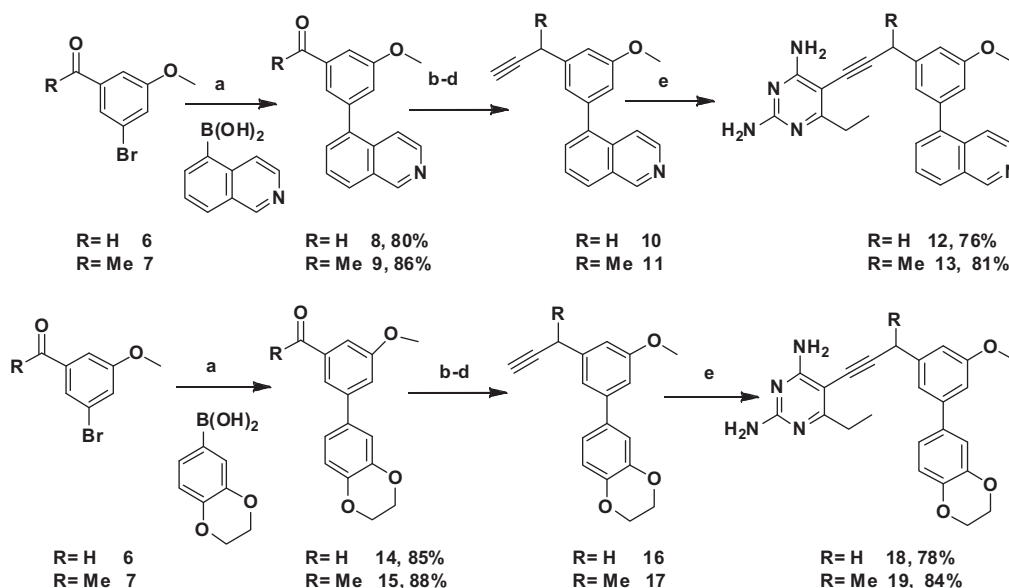
incorporated heteroatom(s). Using Surflex-Dock,¹⁴ approximately 250 compounds derived from commercially available boronic acid

building blocks were docked to the fungal and human structures. Compounds with substituted isoquinoline and benzodioxane ring systems emerged as potential leads. The parent compounds (**12**, **13**, **18**, and **19** in Table 1) were chosen for synthesis in order to make a preliminary evaluation of this new design.

Compounds **12**, **13**, **18**, and **19** were prepared based on analogy to prior routes¹² and involved a key Suzuki coupling between the isoquinoline or benzodioxane boronic acids and the brominated benzaldehyde (**6**) or acetophenone (**7**) to give **8** and **9** in excellent yields (Scheme 1). After completion of the coupling, the aldehyde or methyl ketone was homologated to the corresponding terminal alkynes **10** and **11** through sequential Wittig condensation, hydrolysis and Ohira–Bestmann reaction. The inhibitors (**12**, **13**, **18**, and **19**) were ultimately prepared in high yield by a final Sonogashira coupling with an iodo-pyrimidine.

Evaluation of enzyme inhibition (Table 1) shows that **12**, **13**, **18** and **19** are potent inhibitors of CgDHFR and additionally that **13** and **19** are potent inhibitors of CaDHFR. Thus, the expanded ring system enhanced affinity for the fungal enzymes, as designed. Unfortunately, the compounds also potently inhibit the human form of the enzyme and in fact, lowered the selectivity index relative to the biphenyl compounds. The fact that the docking scores predicted better selectivity than was observed experimentally may point to the difficulty of negative design (selectivity) using algorithms developed for positive design (potency). Although these results indicate that this strategy would not be useful for improving selectivity, it also revealed that the understanding of this region of the active site is incomplete and that these molecules could serve as useful probes to better characterize the dynamic aspects of the active site residues.

In an effort to understand the basis of potency and the diminished selectivity of the compounds with fused ring heterocycles, crystal structures of CgDHFR and CaDHFR bound to NADPH and **18** were determined (PDB IDs: 4H98 and 4H96). Again, the loop residues in the fungal DHFR enzymes show ligand-induced conformational changes. In CgDHFR with benzodioxane **18**, the loop containing Pro63–Phe 66 shows modest displacement by 0.75 Å to more optimally interact with the dioxane moiety as compared to the structure of CgDHFR bound to the biphenyl **1** (Fig. 3A). In CaDHFR, although Pro 63 remains in the same position in the structures with both **1** and **18**, the remainder of the residues in the



Scheme 1. Reagents and conditions: (a) Pd(PPh₃)₂Cl₂, Cs₂CO₃, dioxane, 80 °C; (b) Ph₃P=CHOMe, THF; (c) Hg(OAc)₂, KI, THF/H₂O; (d) dimethyl(1-diazo-2-oxopropyl)phosphonate, K₂CO₃, MeOH; (e) 5-iodo-6-ethyl pyrimidine, Pd(PPh₃)₂Cl₂, CuI, Et₃N, DMF.

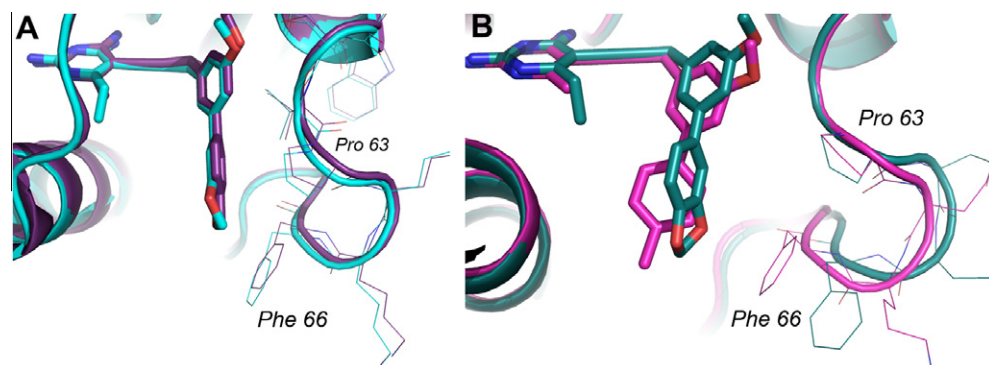


Figure 3. Superposition of structures of (A) CgDHFR bound to **18** (cyan) and **1** (purple) and (B) CaDHFR bound to **18** (green) and **1** (pink).

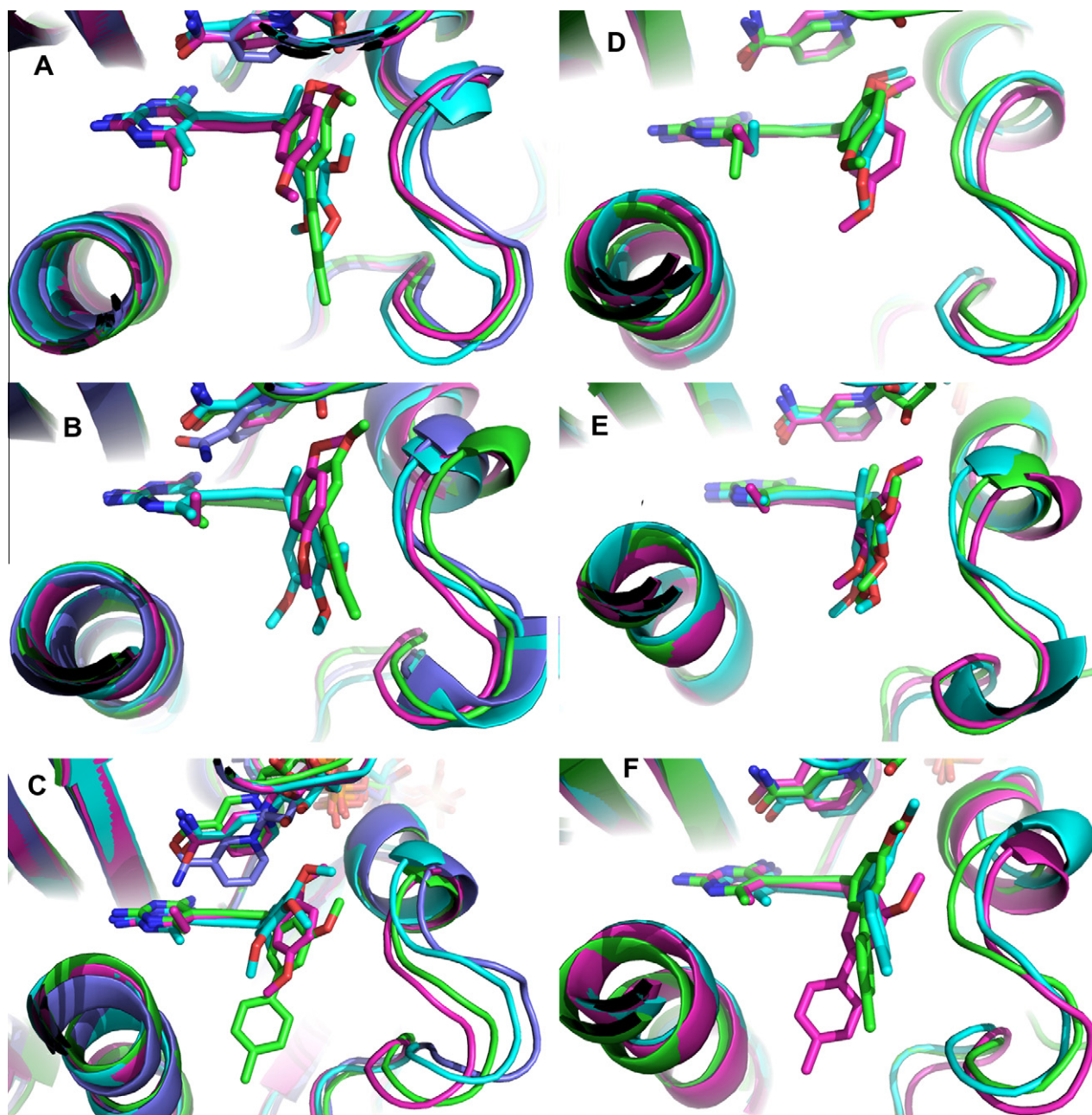


Figure 4. MD analysis by species A–C. (A) huDHFR, (B) CgDHFR and, (C) CaDHFR bound to **20** (pink), **21** (cyan), **1** (green) and in the binary state (purple). MD analysis by ligand, (D–F) huDHFR (green), CgDHFR (cyan) and CaDHFR (pink) bound to (D) **20**, (E) **21** and (F) **1**.

CaDHFR loop (64–66) are significantly displaced by up to 2 Å, driven largely by interactions with Phe 66 (Fig. 3B).

Although it is clear that the loop residues in fungal DHFR show ligand-induced conformational changes, it is not evident whether the human DHFR loop residues show similar dynamics. Therefore, it became essential to evaluate the differential dynamics of the fungal and human loops in order to refine the model for future design work.

In order to assess the dynamics of the loop residues and the degree to which they are influenced by the bound ligand in both fungal and human DHFR enzymes, we carried out free MD simulations inclusive of solvent using ternary and binary (only NADPH bound) complexes. Three compounds (**1**, **20** and **21** in Table 1) representing a spectrum of potency and selectivity for human and fungal DHFR were chosen to probe the loop conformation.

Crystal structures of CgDHFR and CaDHFR bound to compounds **1**, **20** and **21** were used as starting structures; compounds **1**, **20** and **21** were docked to human DHFR. Protein complexes were prepared by assigning bond orders, adding hydrogens, capping termini, deleting all waters, adding missing side chains and optimizing hydrogen bonds.¹⁵ Desmond system builder was used to construct the system for simulation. A periodic boundary box was built by explicitly adding waters, counter ions and salt to simulate physiological conditions. The resulting system was minimized using two stages (restrained and unrestrained) followed by several stages of MD runs to gradually remove any system restraints. The prepared systems were transferred to the Extreme Science and Engineering Digital Environment (www.xsede.org, formerly the TeraGrid). Simulations were run in Desmond with the OPLS force-field for 10 ns. Visualization and analysis focused on the last 9 ns to ensure system equilibrium was achieved prior to production.

Analyzing each species independently reveals that the loop residues appear to adopt ligand-induced conformations. Relative to the loop conformation adopted with **20** in human DHFR (Fig. 4A), the loop is displaced 0.4 Å (as measured from C α of Pro 61) in the structure with **1**, 1.4 Å in the structure with **21** and 1.6 Å in the binary complex. For CgDHFR (Fig. 4B), relative to the loop conformation adopted with **20**, the displacement is 1.2, 0.9, and 1.6 Å, respectively. Lastly, in CaDHFR (Fig. 4C) the same comparison yields displacements of 1.2, 2.3 and 4.3 Å. These results show that the ligand induces significant displacement of the loop residues in all three species.

We next investigated whether a given ligand would induce the same loop conformation across the three different species. Superpositions of the three species bound to the same ligand (Fig. 4D–F) show that the loop residues show minimal displacements, reflecting ligand-induced conformational changes are independent of species. The fact that the ligand drives a specific conformation of the loop, independent of species, implies that selectivity cannot be easily achieved by attempting to induce species-specific steric interference.

Targeting metabolic enzymes such as dihydrofolate reductase in *Candida* spp. has the potential to lead to the development of novel treatment strategies for fungal infections. The analysis of existing crystal structures of *C. albicans* and *C. glabrata* DHFR as well as four new ternary structures presented here highlight that a key loop at the active site undergoes ligand-induced conformational changes. Based on docking results, four new compounds intended to probe the flexibility of the loop were synthesized and found to be potent inhibitors of the pathogenic and, somewhat surprisingly, human enzymes. Crystal structures of one of these compounds bound to the fungal enzymes again emphasized ligand-induced conformational changes. Molecular dynamics simulations with the fungal and human enzymes reveal that the loop undergoes ligand-induced conformational changes that are driven by the ligand, not the species. As the conformation of the loop may not allow the design of selective inhibitors, greater emphasis should be placed instead on residue substitutions.

Acknowledgements

The authors thank the NIH for funding this work (GM067542), the Pittsburgh Supercomputing Center for time to perform the molecular dynamics calculations and Melanie Allen for assistance with enzyme assays.

Supplementary data

Supplementary data associated with this article can be found, in the online version, at <http://dx.doi.org/10.1016/j.bmcl.2013.01.008>.

References and notes

1. Pfaller, M.; Diekema, D. J. *Clin. Microbiol.* **2004**, *42*, 4419.
2. Pfaller, M.; Diekema, D. *Clin. Microbiol. Rev.* **2007**, *20*, 133.
3. Arendrup, M. *Curr. Opin. Clin. Care* **2010**, *16*, 445.
4. Falagas, M.; Roussos, N.; Vardakas, K. *Int. J. Infect. Dis.* **2010**, *14*, e954.
5. Bennett, J. E.; Izumikawa, K.; Marr, K. *Antimicrob. Agents Chemother.* **2004**, *48*, 1773.
6. Bolstad, D.; Bolstad, E.; Frey, K.; Wright, D.; Anderson, A. *J. Med. Chem.* **2008**, *51*, 6839.
7. Liu, J.; Bolstad, D.; Smith, A.; Priestley, N.; Wright, D.; Anderson, A. *Chem. Biol. Drug Des.* **2008**, *15*, 990.
8. Liu, J.; Bolstad, D.; Smith, A.; Priestley, N.; Wright, D.; Anderson, A. *Chem. Biol. Drug Des.* **2009**, *73*, 62.
9. Pelphrey, P.; Popov, V.; Joska, T.; Beierlein, J.; Bolstad, E.; Fillingham, Y.; Wright, D.; Anderson, A. *J. Med. Chem.* **2007**, *50*, 940.
10. Paulsen, J.; Liu, J.; Bolstad, D.; Smith, A.; Priestley, N.; Wright, D.; Anderson, A. *Bioorg. Med. Chem.* **2009**, *17*, 4866.
11. Paulsen, J.; Bendel, S.; Anderson, A. *Chem. Biol. Drug Des.* **2011**, *78*, 505.
12. Viswanathan, K.; Frey, K.; Scocchera, E.; Martin, B.; Swain, P.; Alverson, J.; Priestley, N.; Anderson, A.; Wright, D. *PLoS One* **2012**, *7*, e29434.
13. Cody, V.; Luft, J.; Pangborn, W.; Gangjee, A. *Acta Crystallogr.* **2003**, *D59*, 1603.
14. Jain, A. *J. Med. Chem.* **2003**, *46*, 499.
15. Preparation performed with Maestro preparation wizard (Schrodinger, Inc.), Desmond System builder is distributed through D. E. Shaw Research.